arXiv:1610.03894v1 [hep-ph] 12 Oct 2016

Not-that-heavy Majorana neutrino signals at the LHC.

Lucía Duarte*

Instituto de Física, Facultad de Ingeniería, Universidad de la República

Julio Herrera y Reissig 565,(11300) Montevideo, Uruguay.

Javier Peressutti and Oscar A. Sampayo†

Instituto de Investigaciones Físicas de Mar del Plata (IFIMAR)

CONICET, UNMDP

Departamento de Física,

Universidad Nacional de Mar del Plata

Funes 3350, (7600) Mar del Plata, Argentina

Abstract

We consider the possibility of Majorana neutrinos production at the Large Hadron Collider (LHC) by studying the $pp \to l_i^+ l_j^+ + 2\ jets$ ($l_j \equiv e, \mu$) process which, due to leptonic number violation, is a clear signature for intermediate Majorana neutrino contributions. The interactions between Majorana neutrinos and the Standard Model particles are obtained from an effective lagrangian approach. Majorana neutrinos with masses of a few GeV are long-lived neutral particles, and we take advantage of its measurable decay length: in the same-sign dilepton channel, we exploit this fact imposing cuts that reject the SM background, and analyze the distribution corresponding to the angle between the final leptons, using a forward-backward asymmetry to study the effects of the different gauge invariant operators. We also study the $pp \to l_i^+ \nu\gamma$ process, which is dominant for low m_N masses if tensorial one-loop generated new physics contributions are present. This channel could be observed at the LHC with the aid of non-pointing photons observables and cuts on the displacement between the prompt lepton and the photon.

*Electronic address: lduarte@fing.edu.uy

†Electronic address: sampayo@mdp.edu.ar

I. INTRODUCTION

While the discovery of neutrino oscillations and its interpretation in terms of non-zero neutrino masses remains as the most compelling evidence for the existence of physics beyond the Standard Model, many proposals have been posed to explain the tiny neutrino masses, and the seesaw mechanism stays as one of the most straightforward means for solving this problem [1–6]. The mechanism introduces right handed sterile neutrinos that, as they do not have distinct particle and antiparticle degrees of freedom, can have a Majorana mass term leading to the known masses for the standard neutrinos, as long as the Yukawa couplings between the right handed Majorana neutrinos and the standard ones remain small. The Majorana mass term implies the possibility for lepton number violating (LNV, $\Delta L = 2$) processes involving charged leptons.

The inquiry on the Majorana nature of neutrinos has led to dedicated searches for evidence of LNV at hadron colliders in the very well known same-sign dilepton channel $pp \to l_i^+ l_j^+ + 2\ jets$ [7–20], recently including new production mechanisms [21–23], and the chances to discover heavy Majorana neutrinos in e^+e^-, e^-P, $e^-\gamma$ and $\gamma\gamma$ colliders have been studied [24–33]. Searches for heavy Majorana neutrinos in the ss-dilepton channel are currently being performed at the LHC [34–38].

In the naïve Type-I seesaw scenarios often studied, Yukawa couplings of order $Y \sim 1$, require a Majorana neutrino mass scale of order $M_N \sim 10^{15} GeV$ to account for a light ν mass compatible with the current oscillation data ($m_\nu \sim 0.01 eV$), and this fact leads to the decoupling of the Majorana neutrinos, or to a negligible left-right neutrino mixing $U_{lN}^2 \sim m_\nu / M_N \sim 10^{-14} - 10^{-10}$. Thus, as suggested in [14], the detection of Majorana neutrinos (N) via $\Delta L = 2$ processes, would be a signal of physics beyond the minimal seesaw mechanism. The Majorana neutrino interactions could be best described in a model independent approach based on an effective theory, considering a scenario with only one Majorana neutrino N and negligible mixing with the ν_L.

The effective model we consider in this paper [14] has been tested in the LHC [37, 38] for Majorana neutrino masses above 100 GeV, in events with high transverse momentum objects including two reconstructed leptons and jets, for $\sqrt{s} = 7\ TeV$. The data are found to be in agreement with the expected SM background, leading to limits in the effective couplings and new physics scale for some selected operators. If this kind of sterile neutrino

exists for $m_N < m_W$, the produced jets in the final state $l_i^+ l_j^+ + 2\ jets$ may not pass the cuts required to reduce backgrounds, as pointed out, for example, in ref. [39].

Indeed, for masses m_N around a few GeV the Majorana neutrino we are considering behaves as a long-lived neutral particle, with a measurable decay length. This gives us a new means for probing the effective new physics at this lower mass scale, taking advantage of displaced vertices techniques. Recent works use displaced vertices for studying heavy sterile neutrinos in the LHC [19, 40–43] and future colliders [44, 45].

In our previous work [46] we found that for $m_N \lesssim 30\ GeV$, the dominant neutrino plus photon $N \to \nu\gamma$ decay channel is given by the contribution of effective tensorial operators generated at one-loop level in the unknown underlying ultraviolet theory. As this channel cannot shed light on the Majorana or Dirac nature of heavy neutrinos, we first tackle the LNV same-sign dilepton signals for low Majorana neutrino masses neglecting the one-loop operators contribution. This enables us to test the capability to discern between the different gauge invariant operators contribution to the $pp \to l_i^+ l_j^+ + 2\ jets$ process, using a forward-backward asymmetry, and imposing displaced-vertices cuts that reject the SM background, in a scenario with no one-loop-generated operators contribution.

In spite of not being a LNV signal, a study of the dominant neutrino plus photon decay channel is included in this paper, as it also was found that long-lived neutral radiatively decaying particles like the Majorana neutrino N, could explain the MiniBooNE [47, 48] and SHALON [49] anomalies [46], following sterile neutrino explanations for these experimental puzzles [50]. The radiative $N \to \nu\gamma$ channel can be observed by the signature of an isolated electromagnetic cluster together with missing transverse energy, where the photon originates in a displaced vertex. New physics searches involving displaced photons and missing transverse energy have been performed at the LHC [51, 52], mainly dedicated to SUSY searches, and searches with the same final state: lepton, photon and missing E_T [53].

The paper is organized as follows. In sections I A and I B we review the effective lagrangian approach and the experimental bounds on the effective couplings. In Sec.I C we discuss the distinctive features of the low m_N region for our signals. The same-sign dilepton plus jets process is studied in Sec.II, introducing the displaced leptons distance $L^{l^+l^+}$ and our results for the leptonic forward-backward asymmetry $A_{FB}^{l^+l^+}$. In Sec.III we study the prompt lepton and neutrino plus photon process, presenting the non-pointing photon z_{DCA} and displaced lepton-photon distance $L^{l^+\gamma}$ signal distributions. Our final remarks are given in Sec.IV.

A. Effective model

While most of the recent work has been focused on the investigation of heavy Majorana neutrinos that mix with the SM light neutrinos in the framework of Type-I seesaw scenarios [12, 13], the aim of our approach is to investigate the possible contribution of a heavy Majorana neutrino with negligible mixing to the SM ν_L.

Thus we consider an effective lagrangian in which we include a relatively light right handed Majorana neutrino N as one of the observable degrees of freedom. The effects of the new physics involving one heavy sterile neutrino and the SM fields are parameterized by a set of effective operators $\mathcal{O}_{\mathcal{J}}$ constructed with the standard model and the Majorana neutrino fields and satisfying the $SU(2)_L \otimes U(1)_Y$ gauge symmetry [54].

The effect of these operators is suppressed by inverse powers of the new physics scale Λ, for which we take the value $\Lambda = 1\ TeV$. The total lagrangian is organized as follows:

$$\mathcal{L} = \mathcal{L}_{SM} + \sum_{n=6}^{\infty} \frac{1}{\Lambda^{n-4}} \sum_{\mathcal{J}} \alpha_{\mathcal{J}} \mathcal{O}_{\mathcal{J}}^{(n)} \tag{1}$$

where n is the mass dimension of $\mathcal{O}_{\mathcal{J}}^{(n)}$.

The dominating effects come from dimension 6 operators that can be generated at tree level in the unknown underlying renormalizable theory. Following [14], we start with a rather general effective lagrangian density for the interaction of right handed Majorana neutrinos N with leptons and quarks, including dimension 6 operators. The first subset includes operators with scalar and vector bosons (SVB),

$$\mathcal{O}_{LN\phi} = (\phi^\dagger \phi)(\bar{L}_i N \tilde{\phi}),\ \ \mathcal{O}_{NN\phi} = i(\phi^\dagger D_\mu \phi)(\bar{N}\gamma^\mu N),\ \ \mathcal{O}_{Ne\phi} = i(\phi^T \epsilon D_\mu \phi)(\bar{N}\gamma^\mu e_i) \tag{2}$$

and a second subset includes the baryon-number conserving four-fermion contact terms:

$$\begin{aligned}
\mathcal{O}_{duNe} &= (\bar{d}\gamma^\mu u)(\bar{N}\gamma_\mu l),\ \ \mathcal{O}_{fNN} = (\bar{f}\gamma^\mu f)(\bar{N}\gamma_\mu N),\ \ \mathcal{O}_{LNLe} = (\bar{L}N)\epsilon(\bar{L}l), \\
\mathcal{O}_{LNQd} &= (\bar{L}N)\epsilon(\bar{Q}d),\ \ \mathcal{O}_{QuNL} = (\bar{Q}u)(\bar{N}L),\ \ \mathcal{O}_{QNLd} = (\bar{Q}N)\epsilon(\bar{L}d), \\
\mathcal{O}_{LN} &= |\bar{N}L|^2,\ \ \mathcal{O}_{QN} = |\bar{Q}N|^2
\end{aligned} \tag{3}$$

where e_i, u_i, d_i and L_i, Q_i denote, for the family labeled i, the right handed $SU(2)$ singlet and the left-handed $SU(2)$ doublets, respectively.

One can also consider operators generated at one-loop level in the underlying full theory, whose coefficients are naturally suppressed by a factor $1/16\pi^2$[14, 55]:

$$\begin{aligned} \mathcal{O}^{(5)}_{NNB} &= \bar{N}\sigma^{\mu\nu}N^c B_{\mu\nu}, \\ \mathcal{O}_{NB} = (\bar{L}\sigma^{\mu\nu}N)\tilde{\phi}B_{\mu\nu}, &\qquad \mathcal{O}_{NW} = (\bar{L}\sigma^{\mu\nu}\tau^I N)\tilde{\phi}W^I_{\mu\nu}, \\ \mathcal{O}_{DN} = (\bar{L}D_\mu N)D^\mu\tilde{\phi}, &\qquad \mathcal{O}_{\bar{D}N} = (D_\mu\bar{L}N)D^\mu\tilde{\phi}\ . \end{aligned} \tag{4}$$

In this paper we study the well known same-sign dilepton (ss-dilepton) Majorana neutrino signal $pp \to l_i^+ l_j^+ jj$ schematically depicted in Fig.2, and the new $pp \to l_i^+ \nu\gamma$ neutrino plus photon channel shown in Fig.7. In order to obtain the cross sections for the above processes, we derive the effective lagrangian terms involved in the calculations, taking the scalar doublet after spontaneous symmetry breaking as $\phi = \begin{pmatrix} 0 \\ \frac{v+h}{\sqrt{2}} \end{pmatrix}$, with h being the Higgs field.

For the production vertex I in Figs.2 and 7, and the decay vertex II in Fig.2, we have tree-level generated contributions from the effective lagrangian coming from (2), related to the spontaneous symmetry breaking process, and 4-fermion contributions from (3):

$$\begin{aligned} \mathcal{L}^{tree-level}_{eff} &= \frac{1}{\Lambda^2}\Big\{-\frac{m_W v}{\sqrt{2}}\alpha^{(i)}_W\, W^{\dagger\,\mu}\,\overline{N}_R\gamma_\mu e_{R,i} + \alpha^{(i)}_{V_0}\bar{d}_{R,i}\gamma^\mu u_{R,i}\overline{N}_R\gamma_\mu e_{R,i} + \\ &\quad \alpha^{(i)}_{S_1}(\bar{u}_{L,i}u_{R,i}\overline{N}\nu_{L,i} + \bar{d}_{L,i}u_{R,i}\overline{N}e_{L,i}) + \alpha^{(i)}_{S_2}(\bar{\nu}_{L,i}N_R\bar{d}_{L,i}d_{R,i} - \bar{e}_{L,i}N_R\bar{u}_{L,i}d_{R,i}) + \\ &\quad \alpha^{(i)}_{S_3}(\bar{u}_{L,i}N_R\bar{e}_{L,i}d_{R,i} - \bar{d}_{L,i}N_R\bar{\nu}_{L,i}d_{R,i}) + h.c.\Big\} \end{aligned} \tag{5}$$

where the sum over the families i is understood and the constants $\alpha^{(i)}_{\mathcal{J}}$ are associated to specific operators according to

$$\alpha^{(i)}_W = \alpha^{(i)}_{Ne\phi},\ \alpha^{(i)}_{V_0} = \alpha^{(i)}_{duNe},\ \ \alpha^{(i)}_{S_1} = \alpha^{(i)}_{QuNL},\ \alpha^{(i)}_{S_2} = \alpha^{(i)}_{LNQd},\ \ \alpha^{(i)}_{S_3} = \alpha^{(i)}_{QNLd}\ . \tag{6}$$

For the $N \to \nu\gamma$ decay vertex II in Fig.7, the considered lagrangian terms are generated by one-loop level tensorial operators:

$$\mathcal{L}^{1-loop}_{eff} = \frac{-i\sqrt{2}v}{\Lambda^2}(\alpha^{(i)}_{L_1}c_W + \alpha^{(i)}_{L_3}s_W)(P^{(A)}_\mu\ \bar{\nu}_{L,i}\sigma^{\mu\nu}N_R\ A_\nu). \tag{7}$$

where $-P^{(A)}$ is the 4-moment of the outgoing photon and a sum over the family index i is understood again. The coupling constants $\alpha^{(i)}_{L_{1,3}}$ are associated to the specific operators:

$$\alpha^{(i)}_{L_1} = \alpha^{(i)}_{NB},\ \ \alpha^{(i)}_{L_3} = \alpha^{(i)}_{NW}$$

The complete lagrangian is presented in an appendix in [56].

The effective operators can be classified by their structure into *scalar*, *vectorial* and *tensorial*. The scalar and vectorial operators contributing to the studied processes are those appearing in (5) with couplings named $\alpha_{S_{1,\ 2,\ 3}}$ and $\alpha_{W,\ V_0}$ respectively. They play a role in the production and decay vertices for the $pp \to l_i^+ l_j^+ + 2\ jets$ process, and only in the production vertex for the $l_i^+ \nu\gamma$ channel. The one-loop tensorial operators in (7) drive the $N \to \nu\gamma$ decay.

B. Effective coupling bounds summary

Recent reviews [30, 57–60] summarize in general phenomenological approaches the existing experimental bounds, considering low scale minimal seesaw models, parameterized by a single heavy neutrino mass scale M_N and a light-heavy mixing U_{lN}, with l indicating the lepton flavor. In previous works [46, 56] we have presented in detail the way in which we take into account existing constraints on processes like neutrinoless double beta decay ($0\nu\beta\beta$), electroweak precision data (EWPD), LNV rare meson decays as well as direct collider searches, including Z decays. In order to put bounds for the effective couplings, we take into account existing experimental constraints on sterile-active neutrino mixings, relating the U_{lN} mixings in Type-I seesaw models [12, 13] with our effective couplings by the relation

$$U_{lN}^2 \simeq \left(\frac{\alpha v^2}{2\Lambda^2}\right)^2 . \tag{8}$$

For the couplings involving the first fermion family the most stringent are the $0\nu\beta\beta$-decay bounds obtained by the KamLAND-Zen collaboration [61]. Following the treatment made in [56, 57, 62], they give us an upper limit $\alpha_{0\nu\beta\beta}^{bound} \leq 3.2 \times 10^{-2} \left(\frac{m_N}{100\ GeV}\right)^{1/2}$. Concerning the second fermion family, for sterile neutrino masses $2\ GeV \lesssim m_N \lesssim 10\ GeV$ the upper limits come from the DELPHI collaboration [63]. Considering $\Omega_{ll'} = U_{lN} U_{l'N}$ as in [13], we obtain the bound $\alpha_{DELPHI}^{bound} \lesssim 2.3$. The Belle [64] and LHCb [65] collaborations also find competitive upper limits in the $2\ GeV \lesssim m_N \lesssim 5\ GeV$ region. These results tough depend heavily on the considered decay modes for the sterile N [66–70]. The bound from Belle is still the most stringent, giving a value $\alpha_{Belle}^{bound} \lesssim 0.3$. For higher masses, in the range $m_W \lesssim m_N$ the upper limits come from EWPD as radiative lepton flavor violating (LFV) decays as $\mu \to e\gamma$ [57, 60, 71, 72] giving a bound $\alpha_{EWPD}^{bound} \leq 0.32$.

In order to simplify the discussion, for the numerical evaluation we only consider the

most stringent bounds, taking the couplings associated to the operators that contribute to the $0\nu\beta\beta$-decay for the first family as restricted by the corresponding bound $\alpha^{bound}_{0\nu\beta\beta}$, and the other constants are restricted to the value $\alpha^{bound} \leq 0.3$. For the 1-loop generated operators we consider the coupling constant as $1/(16\pi^2)$ times the corresponding tree-level coupling: $\alpha^{1-loop} = \alpha^{tree}/(16\pi^2)$. Thus, for example, for the operator $\mathcal{O}_{NW}$, which contributes to $0\nu\beta\beta$ we have

$$\alpha^{(1)}_{L_3} = \frac{1}{16\pi^2}\alpha^{bound}_{0\nu\beta\beta}.$$

C. Low m_N kinematic features

As we mentioned in the introduction, Majorana neutrinos with masses of a few GeV are found to be long-lived neutral particles that could be searched for in the LHC with displaced vertices techniques. In this paper we exploit this long decay length in order to search for the production of Majorana neutrinos.

In higher m_N regions, the same-sign dilepton (l^+l^+jj) signal has been thoroughly studied in colliders and, as we mentioned in the introduction, this signal has been studied in the effective framework we consider here [14], and searched for in the LHC [37, 38] for m_N above $100GeV$. Up to now, all LHC searches for heavy Majorana neutrinos [34–38] in these final states are performed without considering the possibility of a sufficiently long heavy neutrino lifetime making the decay vertex to be displaced from the production point.

The decay length of the Majorana neutrino, and its flight direction in the lab frame can be determined as:

$$\vec{l}_N = \frac{\vec{k}_N}{|\vec{k}_N|}\tau_N\beta_N = \frac{\vec{k}_N}{|\vec{k}_N|}\frac{\left((E_N/m_N)^2-1\right)^{1/2}}{\Gamma_N} \tag{9}$$

where k_N is the N momentum, $E_N^2 = |\vec{k}_N|^2 + m_N^2$ and Γ_N is the decay width.

In order to make a preliminary survey we study the same-sign dileptons plus jets and the lepton and neutrino plus photon channels making a parton level Monte Carlo simulation with the RAMBO [73] routine. The effective new physics energy scale Λ in (1) is taken to be $\Lambda = 1\ TeV$, and the CM energy of the hard processes $\sqrt{s} \leq \Lambda$, to insure the validity of the effective Lagrangian approach. The numerical values for the effective couplings are taken as explained in Sec.I B.

The measurable decay length of the few-GeV mass Majorana neutrino will be exploited

in this paper considering two distinct observables: for the ss-dilepton signal, we find the vertex displacement can be measured by obtaining the distance between the traces of both outgoing leptons, a prompt one coming from the N production vertex, and the other in the decay vertex. For the neutrino plus photon channel, we consider the distance between the prompt outgoing lepton and the displaced photon traces, and also the non-pointing photon observables defined in recent new physics searches in ATLAS [51, 52].

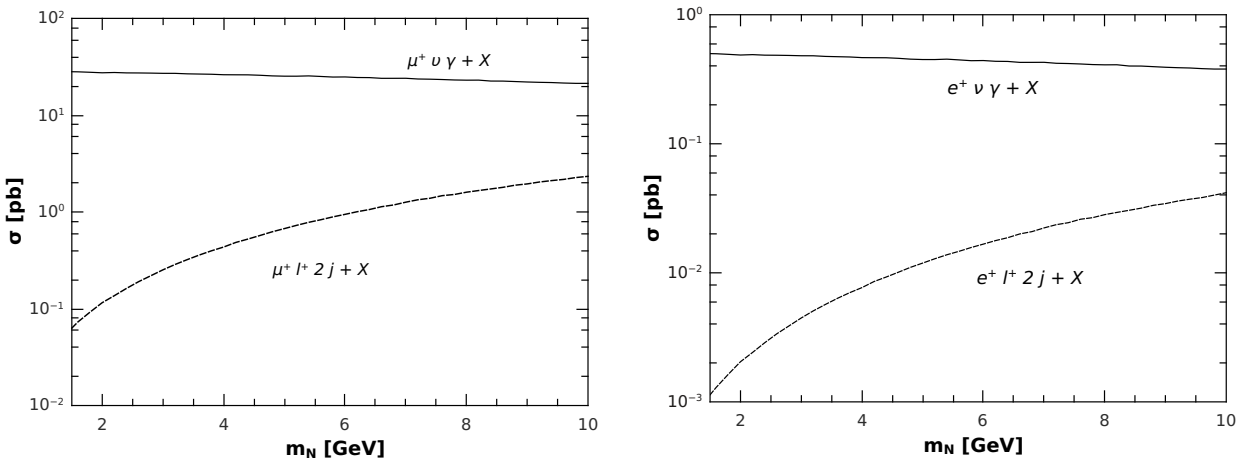

(a) Muon channel

(b) Electron channel

FIG. 1: Total cross sections for the $pp \to l^+\nu\gamma + X$ and $pp \to l^+l^+ + 2\ j + X$ processes.

In the effective framework we are working with, the dominant decay channel in the few-GeV m_N mass region is the $N \to \nu\gamma$. Considering an on shell N production, the cross section for the ss-dilepton process can be written as the product of the production cross section by the decay channel branching ratio: $\sigma(pp \to lljj) \simeq \sigma(u\bar{d} \to lN)Br(N \to ljj)$. Taking into account non-zero values for the scalar, vectorial and tensorial couplings, the cross sections for the l^+l^+jj and the $l^+\nu\gamma$ final states are shown in Fig.1.

As the radiative N-decay channel completely dominates the low mass region and is driven by tensorial one-loop operators, for the study of the LNV same-sign dileptons plus jets signal, we fix $\alpha_{1-loop} = 0$, and focus our interest in distinguishing the effects of the vectorial and scalar operators on the signal, as it is not sensitive to the tensorial operators effect.

In Fig.1 one can also appreciate the diminishing effect of the $\alpha_{0\nu\beta\beta}^{bound}$ value on the $l^+ = e^+$ channel: the cross section for the second family $l^+ = \mu^+$ is appreciably higher, due to the

more relaxed bound α_{Belle}^{bound}.

II. SAME SIGN DILEPTON SIGNAL

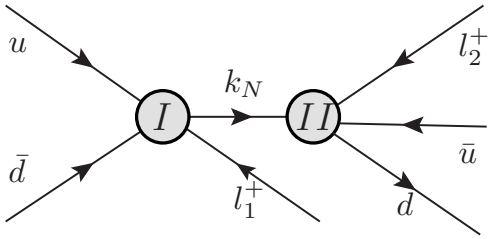

FIG. 2: Diagrams contributing to the process $pp \to l^+ l^+ jj$.

Using the effective lagrangian in Eq.(5), we calculate the cross section for the production of the Majorana neutrino according to the parton hard processes shown in Fig.2.

The corresponding amplitude can be written as the product of the production and decay processes:

$$\begin{aligned}\mathcal{M} \quad &= \frac{-im_N}{\Lambda^4} P_N(k_N^2) \Big\{ \Pi_W(q_2^2) \alpha_W^{(i)}\, \bar{u}(l_u)\gamma_\nu P_R v(l_d)\bar{u}(l_2)\gamma^\nu + \alpha_{V_0}^{(i)}\, \bar{u}\gamma_\nu P_L v(l_d)\bar{u}(l_2)\gamma^\nu + \\ &\alpha_{S_1}^{(i)}\, \bar{u}(l_u) P_R v(l_d)\bar{u}(l_2) - \alpha_{S_2}^{(i)}\, \bar{u}(l_u) P_L v(l_d)\bar{u}(l_2) + \\ &\alpha_{S_3}^{(i)}\, \bar{u}(l_2) P_L v(l_d)\bar{u}(l_u) \Big\} \otimes \Big\{ -\Pi_W(q_1^2) \alpha_W^{(i)}\, \gamma_\mu P_R v(l_1)\bar{v}(p_d)\gamma^\mu P_L u(p_u) + \\ &\alpha_{V_0}^{(i)}\, \gamma_\mu P_R v(l_1)\bar{(}p_d)\gamma^\mu P_R u(p_u) + \alpha_{S_1}^{(i)}\, P_L v(l_1)\bar{v}(p_d) P_R u(p_u) - \\ &\alpha_{S_2}^{(i)}\, P_L v(l_1)\bar{v}(p_d) P_L u(p_u) + \alpha_{S_3}^{(i)}\, P_L u(p_u)\bar{v}(p_d) P_L v(k_1) \Big\}, \end{aligned} \tag{10}$$

where l_1 and l_2 are the 4-moments of the final leptons, p_u and p_d are the 4-moments of the initial quarks and, l_u and l_d stand for the 4-moments of the final quarks. The W propagator is Π_W, k_N is the 4-moment of the intermediate Majorana neutrino, and P_N its propagator.

Taking the center of mass energy $\sqrt{s} = 14$ TeV, $\hat{\sigma}$ and $\hat{s}$ to be the parton level scattering cross section and squared center of mass energy, and x_1 and x_2 the usual deep inelastic scaling variables, we obtain

$$\sigma(pp \to l^+ l^+ + 2jets) = \int_{x_m}^1 \int_{x_m/x_1}^1 dx_1 dx_2 (f_u(x_1) f_{\bar{d}}(x_2) + f_u(x_2) f_{\bar{d}}(x_1)) \hat{\sigma}_i(x_1 x_2 s) \tag{11}$$

where the minimum value for x_1 and x_2 is $x_m = m_N^2/s$ and the function $f_q(x)$ represents the $q(x)$ parton distribution function (PDF).

In view of the discussion given in the introduction, we study the few-GeV m_N region for the ss-dilepton signal taking into account the separate effects of the scalar and vectorial operators, and considering the tensorial operators contribution not to be present. To see the effects from the scalar operators we set the coupling constants corresponding to the vector operators α_W and α_{V_0} equal to zero. Similarly, to study the contribution from the class of vector operators we set the couplings α_{S_1}, α_{S_2} and α_{S_3} equal to zero. Throughout this section we present our numerical results summing over the final leptons possibilities ($l_1^+ l_2^+ = e\mu$, μe, ee, $\mu\mu$).

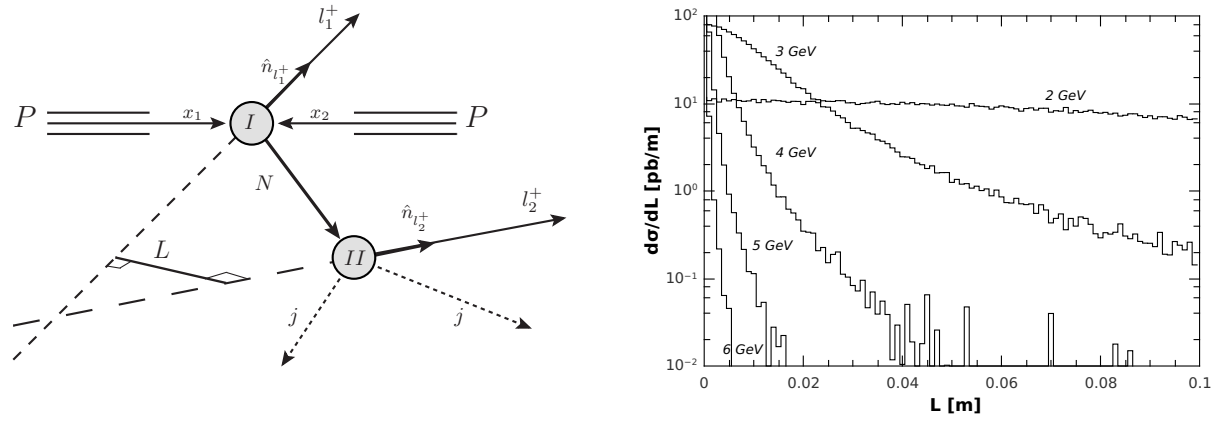

(a) Schematic representation of the distance $L^{l^+l^+}$ between the final leptons directions

(b) Differential $L^{l^+l^+}$ distribution for different m_N values. Scalar and vectorial operators are included.

FIG. 3: $L^{l^+l^+}$ definition and differential distribution.

As the considered signal is a LNV process, it is strictly forbidden in the SM, and the background always involves additional light neutrinos in the final state that escape the detectors as missing energy. The SM backgrounds have been extensively discussed in the literature [12, 13, 16, 20], and in recent experimental searches [34, 35].

The background for these searches can be classified into prompt leptons, charge-flip opposite-sign dileptons and misidentified leptons. The first are SM events resulting in two genuine same-sign leptons, including diboson production (WZ, ZZ) giving ss-dileptons when both Z and W decay leptonically and one lepton from Z decay cannot be isolated or is missed out of the detector coverage, $t\bar{t}$-plus boson ($t\bar{t}W$, $t\bar{t}W$, $t\bar{t}Z$) processes contributing to the signal when the tops decay hadronically and the bosons decay leptonically, triboson ($W^\pm W^\pm W^\mp$), double W-sstrahlung ($WWjj$) and double parton scattering ($qq' \to W$). The

charge-flip events originate in opposite-sign dileptons signals in which an electron undergoes bremsstrahlung in the tracker volume and the associated photon decays into en e^+e^- pair, and the opposite sign electron is misidentified as the primary electron if it carries a large fraction of the original electron's energy. This effect is negligible for muons. The last group includes objects misidentified as prompt leptons, originated in B-hadrons decays, light quark or gluon jets and photon conversions, and mainly $t\bar{t}$ in which a top quark yields a prompt isolated lepton ($t \to Wb \to l\nu b$) and the other same charge lepton arises from b quark decay or a jet misidentified as an isolated prompt lepton. This is the dominant background for the $m_N < m_W$ region [13, 34], and it cannot be easily eliminated in the few-GeV m_N region, as the cuts imposed on the final leptons p_T in order to reject those coming from b decays can also affect the signal. Distributions on the invariant mass of the l_2^+jj system $M(l_2^+jj) \sim m_N$ could help to distinguish the signal from backgrounds [18, 39].

Taking into account the vertex displacement could help reduce the background, and that is why we study this very interesting feature for the low mass region. Recent LHC searches exploiting the long-lived particles displaced vertex feature in final states with charged leptons and jets [74–77] originally intended for SUSY particles [78] are currently being used for studying models with right handed massive neutrinos [40].

We calculate the distance between the traces of the charged leptons, which, almost always, is different from zero since the vertices are displaced. A sketch in Fig. 3a shows the $L^{l^+l^+}$ distance definition.

In our parton level MC-simulation, the distance between the straight line containing the flight direction of the prompt lepton produced in the primary vertex and the one for the displaced secondary lepton can be found as the length of the segment orthogonal to and crossing both traces: $\hat{n}_{l_1^+}$ and $\hat{n}_{l_2^+}$ in Fig. 3a. This line has direction $\hat{n} = \hat{n}_{l_1^+} \times \hat{n}_{l_2^+}/|\hat{n}_{l_1^+} \times \hat{n}_{l_2^+}|$ and the distance $L^{l^+l^+}$ can be calculated as $L^{l^+l^+} = \hat{n} \cdot \vec{l}_N$, with the definition given in (9).

The distribution of the signal distances between the lepton's fly directions is shown in Fig.3b for various few-GeV m_N masses. In order to reject the prompt ss-dilepton background, we set this cut up to $L^{l^+l^+} = 1mm$, which is approximately the precision of the detector, discarding events for which the distance between the traces of the final leptons is less than $1mm$. In this way, we conveniently eliminate the background, since the distance between the traces would be zero if this final state (up to additional non-detectable neutrinos) comes from standard interactions. In Fig.4 we show the scalar and vectorial operators

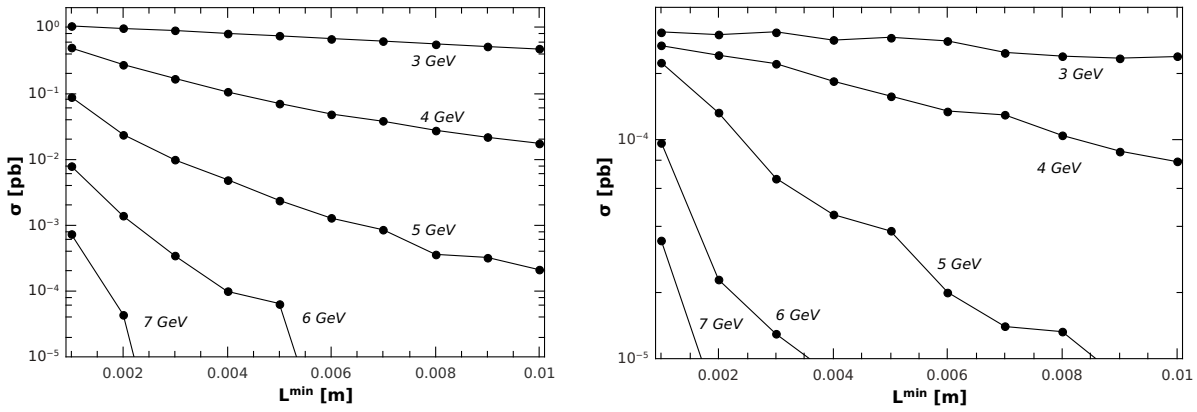

(a) Vectorial (b) Scalar

FIG. 4: Contribution of the vectorial and scalar operators to the cross section for different m_N values as a function of the cut in $L_{min}^{l^+l^+}$.

contribution to the ss-dilepton cross section, for different m_N values, as a function of the cut in the minimal displacement distance $L_{min}^{l^+l^+}$.

Once the displacement between the Majorana production and decay vertices is used to reduce the few-GeV m_N region background, we are interested in testing the separated contributions of the vectorial and scalar operators to the process, in order to obtain information about the kind of new physics behind these effects.

Using the angular distribution $d\sigma/d\cos\theta$ where θ is the angle between the outgoing leptons, we construct a forward-backward asymmetry $A_{FB}^{l^+l^+}$ as a function of the number of events in each hemisphere:

$$A_{FB}^{l^+l^+} = \frac{N_+ \ - \ N_-}{N_+ \ + \ N_-} \tag{12}$$

where N_+ is the number of events with an angle in the interval $0 \leq \theta \leq \pi/2$ and N_- the number of events with $\pi/2 \leq \theta \leq \pi$. This asymmetry does not require the prompt lepton assignment needed for calculating the usual A_{FB} for the underlying production process $pp \to l^+N$, also avoiding the identical colliding beams problem [14].

As can be seen in Fig.5, where we show the angular distribution for a mass of $m_N = 5GeV$, the contributions from both the scalar and vector operators lead to an unbalance. In order to estimate the chances of disentangling the contributions corresponding to the scalar and vector classes of operators, we study the angular asymmetry $A_{FB}^{l^+l^+}$, taking into account the

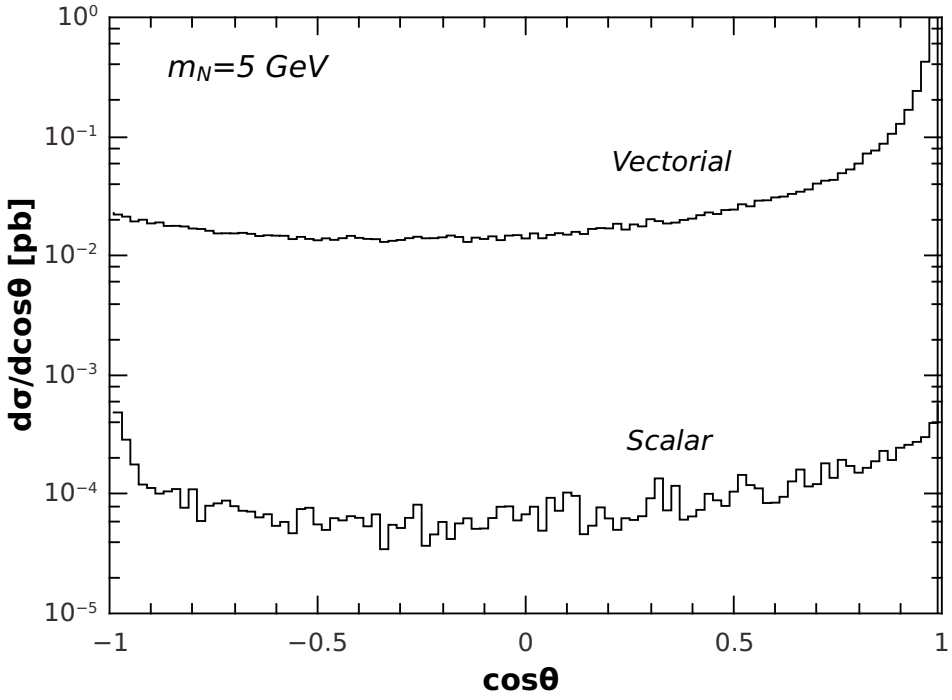

FIG. 5: Angular distribution of the final leptons for $m_N = 5$ GeV and for the contribution of the vectorial and scalars operators

.

error

$$\Delta A_{FB}^{l^+l^+} = \sqrt{\left(\frac{\partial A_{FB}^{l^+l^+}}{\partial N_+}\right)^2 (\Delta N_+)^2 + \left(\frac{\partial A_{FB}^{l^+l^+}}{\partial N_-}\right)^2 (\Delta N_-)^2}. \tag{13}$$

Assuming the number of events to be Poisson distributed, we write

$$\Delta N_+ = \sqrt{N_+} \text{ and } \Delta N_- = \sqrt{N_-} \tag{14}$$

and a straightforward calculation leads to

$$\Delta A_{FB}^{l^+l^+} = \sqrt{\frac{1-(A_{FB}^{l^+l^+})^2}{N_+ + N_-}}. \tag{15}$$

The results for the $A_{FB}^{l^+l^+}$ observable for the vectorial and scalar operators cases are shown in Figs. 6a and 6b. We find that for the scalar set of operators the asymmetry is compatible with zero, but the vectorial set shows a clear effect, different from zero, by several standard deviations. All this figures include the $L_{min}^{l^+l^+} > 1mm$ cut.

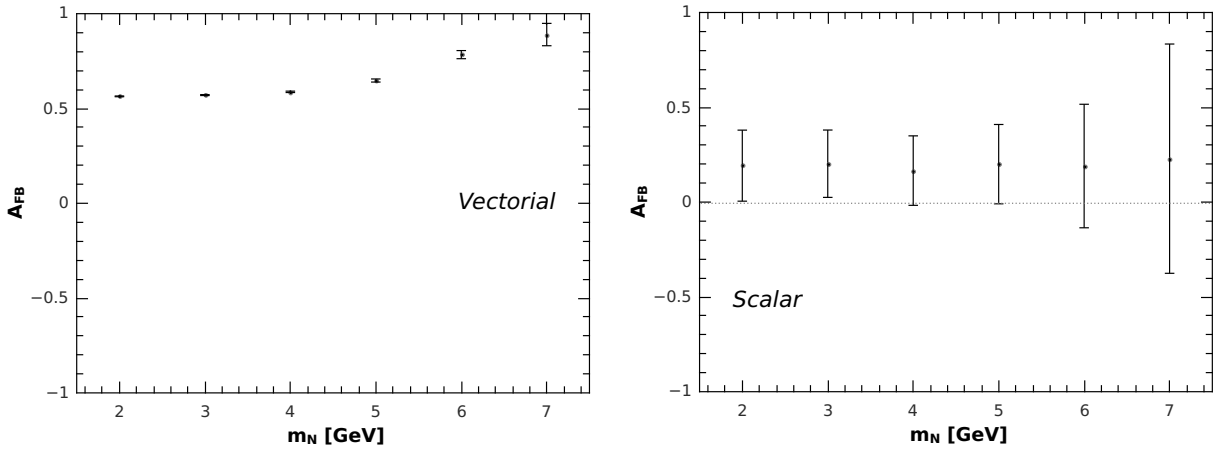

(a) Contribution of the Vectorial Operators.

(b) Contribution of the Scalar Operators.

FIG. 6: Asymmetry in the angular distribution between the final leptons, with the errors estimates as defined in the text.

III. PROMPT LEPTON AND DISPLACED PHOTON PLUS MISSING E_T SIGNAL

As we found in [46], the $N \to \nu\gamma$ decay channel dominates the low m_N region and is driven by one-loop generated tensorial operators. If one includes these in the N decay width calculation, this decay mode would overshadow the ss-dilepton signal. So in the case that new physics involving tensorial modes is present, in this section we explore the chances to observe the $pp \to l^+\nu\gamma$ process in the LHC.

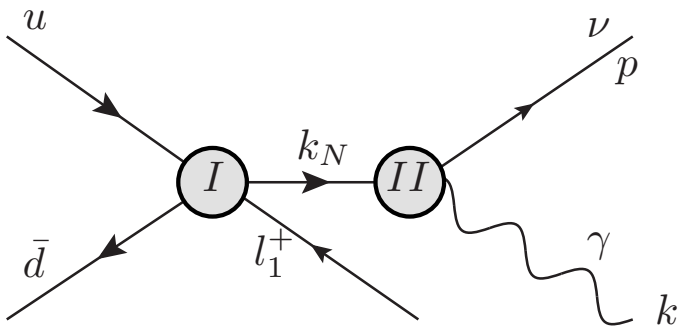

FIG. 7: Schematic momenta in Eqs.(16) and (17).

The cross section for the production and decay of the heavy Majorana neutrino hard process we study can be written as:

$$\hat{\sigma}_{u\bar{d}\to l^+\nu\gamma}(\hat{s}) = \int \frac{1}{2\hat{s}} \overline{|\mathcal{M}|}^2 d\Phi_3$$

Here the squared scattering amplitude in the narrow width approximation is [79]

$$\overline{|\mathcal{M}|}^2 = \frac{\pi}{2\Gamma_N m_N} \delta(k_N^2 - m_N^2) |\mathcal{M}^I|^2 |\mathcal{M}^{II}|^2$$

with the amplitude for the production vertex I in Fig.7 being

$$\begin{aligned} |\mathcal{M}^I|^2 \;=\; & \frac{4}{\Lambda^4}\Big[(l_1.k_N)(p_d.p_u)[\alpha_{S_1}^{(i)2} + \alpha_{S_2}^{(i)}(\alpha_{S_2}^{(i)} - \alpha_{S_3}^{(i)})] \\ & +(l_1.p_u)(p_d.k_N)[\alpha_{S_2}^{(i)}\alpha_{S_3}^{(i)} + 4\alpha_{V_0}^{(i)2}] \\ & +(l_1.p_d)(p_u.k_N)[\alpha_{S_3}^{(i)}(\alpha_{S_3}^{(i)} - \alpha_{S_2}^{(i)}) + 4\alpha_W^{(i)2}|\Pi_W|^2]\Big] \end{aligned} \tag{16}$$

(i is the family index for the final charged anti-lepton l_1^+) and the amplitude for the decay vertex II being

$$|\mathcal{M}^{II}|^2 = \frac{16v^2}{\Lambda^4}\Big[(k.p)^2(\alpha_{L_1}^{(j)}c_W + \alpha_{L_3}^{(j)}s_W)\Big] \tag{17}$$

where $j = 1, 2$ is the family index for the final neutrino.

The background for the $l^+\nu\gamma$ final state has been studied in SUSY searches in events with a photon, a lepton and missing transverse momentum at the LHC [53] for high momentum regions and considering signals where all final particles are produced promptly. It is classified as misidentified photons or leptons and SM-electroweak background. The first arises when electrons or jets are misidentified as photons and comes from events where a photon decays into an e^+e^- pair and an electron fails to register track seeds due to detector inefficiencies, or a jet is misidentified as a photon when a large fraction of its energy is carried by mesons decaying into photons. Misidentified leptons are reconstructed leptons not arising from W or Z boson decays, and come primarily from heavy-flavor quark decays and hadrons misidentified as leptons. The SM-electroweak background is dominated by $Z, W - \gamma$ events that have the same signature as the signal events: a photon, a lepton and missing transverse energy (E_T^{miss}) from neutrinos. In the case of the dominant SM-electroweak background, leptons arise mostly from $W \to \nu l$ decays, and the E_T^{miss} peaks nearly at $m_W/2$. In our case, for few-GeV m_N this background could be reduced imposing a cut on the $\nu - \gamma$ system transverse mass $M_T \lesssim m_N$ as defined in [53]. Also, the invariant mass of the $e\gamma$ system can

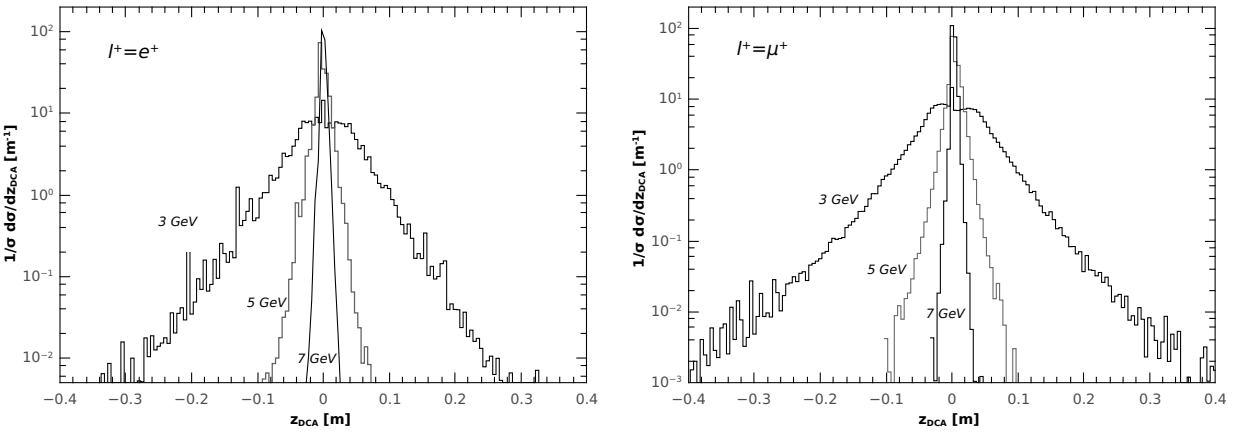

(a) (b)

FIG. 8: z_{DCA} distribution for the $l^+\nu\gamma$ channel.

be required to be different from the nominal Z boson mass, to reduce the background in the $l^+ = e^+$ channel.

For our signal, the smoking gun for the production and flight of the N is its decay length, that leads to a finite separation between the primary and secondary vertex. We are mostly interested in exploiting this distinctive displaced vertex feature, in this case measuring the distance between the prompt lepton track and the displaced photon flight direction, in order to reduce the backgrounds in the low m_N region.

In the LHC, observables using non-pointing photons have been defined and new physics searches were performed involving photons originating from a displaced vertex due to the decay of a long-lived particle into a photon and an invisible particle. This non-pointing photons and E_T^{miss} final state searches [51, 52] are oriented to the discovery of long-lived SUSY particles, but as is the case for this work, could serve the purpose of discovering heavy Majorana neutrinos as well. The analysis technique developed exploits the capabilities of the ATLAS electromagnetic calorimeter to make precise measurements of the flight direction of photons. This direction can be determined by measuring precisely the lateral and the longitudinal positions of the photon-originated shower in the front and middle layers of the EM calorimeter. The variable used as a measure of the degree of non-pointing of the photon is called z_{DCA}, the difference between the z coordinate of the photon extrapolated back to its distance of closest approach (DCA) to the beamline (i.e. $x = y = 0$) and z_{PV}, the z coordinate of the primary vertex [80].

The distance of closest approach of the displaced photon can be calculated using the decay length of the Majorana neutrino defined in (9). Taking $z_{PV} = 0$, in Fig.8 we plot the normalized differential cross section as a function of the distance of closest approach z_{DCA} for the $l^+ = e^+, \mu^+$ channels.

We find our signal leads to z_{DCA} values comparable to those measured in ATLAS [51, 52] (for a very different studied signal consisting of a diphoton final state) and could be searched for, with the aid of other m_N-dependent mentioned cuts suitable for our signal's final state.

Indeed, as suggested in Sec.II, cuts on the displacement distance $L^{l^+\gamma}$ between the prompt lepton and the displaced photon traces could also be implemented, helping to reduce the backgrounds. In Fig.9 we show the normalized differential cross section of the signal for the $l^+ = e^+, \mu^+$ channels as a function of the displacement distance $L^{l^+\gamma}$ defined equivalently as in Sec.II, for different Majorana neutrino masses. We find a cut $L^{l^+\gamma} > 10mm$ would not

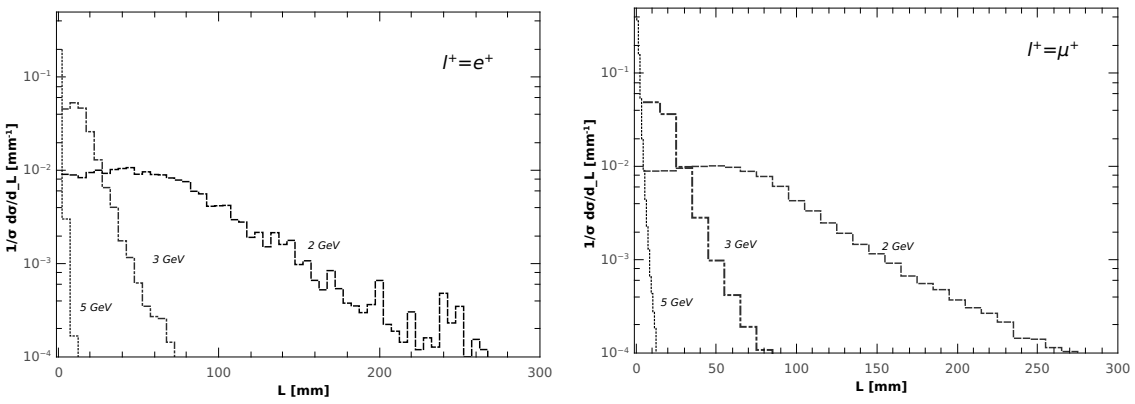

(a) (b)

FIG. 9: $L^{l^+\gamma}$ differential distribution for the $l^+\nu\gamma$ channel.

seriously affect our signal in both flavor charged lepton channels, for m_N up to $5GeV$.

IV. FINAL REMARKS

In this work we study the effects of a heavy sterile Majorana neutrino in the processes $pp \to l_i^+ l_j^+ jj$ and $pp \to l_i^+ \nu\gamma$ in the LHC, modeling the N interactions with the standard particles by an effective lagrangian. As the effective model we consider has already been tested in the LNV ss-dilepton signal for Majorana masses over a hundred GeV, and in fact the

model predicts a low mass N behaves as a long-lived neutral particle with a detectable decay length, in this paper we focus on the complementary study of the ss-dilepton channel for low m_N, exploiting displaced vertices observables to diminish the backgrounds. As for a few-GeV m_N masses the dominant decay channel for the N is $N \to \nu\gamma$, driven by tensorial one-loop generated operators, for the study of the ss-dilepton signal we assume the new physics does not involve tensorial contributions, and study the differences between the vectorial and scalar operators using a forward-backward asymmetry in the angle between the outgoing leptons. Making a statistical analysis we find the contributions from the two operators groups could be distinguished, and the vectorial operators give an asymmetry clearly distinct from zero. Including all the operators contributions we study the dominant low m_N regime $pp \to l_i^+ \nu\gamma$ process, finding the signal distribution in the non-pointing photon observable z_{DCA} could allow for the discovery of the signal in the LHC, with the aid of cuts in the displacement between the prompt lepton and the outgoing photon to reject the backgrounds.

Our encouraging findings suggest to deepen this preliminary parton level study in order to accurately model the signals and backgrounds in the LHC with Monte Carlo simulations including hadronization and detector simulation techniques. The not-that-heavy Majorana neutrinos could be discovered at the LHC in the case the triggers and analysis for Run II dedicated searches keep reconstruction thresholds sufficiently low to efficiently tag displaced vertices form signal processes.

Acknowledgments

We thank CONICET (Argentina) and Universidad Nacional de Mar del Plata (Argentina); and PEDECIBA, ANII, and CSIC-UdelaR (Uruguay) for their financial supports.

---

[1] P. Minkowski, Phys.Lett. **B67**, 421 (1977).

[2] R. N. Mohapatra and G. Senjanovic, Phys.Rev.Lett. **44**, 912 (1980).

[3] T. Yanagida, Prog.Theor.Phys. **64**, 1103 (1980).

[4] M. Gell-Mann, P. Ramond, and R. Slansky, Conf.Proc. **C790927**, 315 (1979), 1306.4669.

[5] J. Schechter and J. W. F. Valle, Phys. Rev. **D22**, 2227 (1980).

[6] B. Kayser, F. Gibrat-Debu, and F. Perrier, World Sci.Lect.Notes Phys. **25**, 1 (1989).

[7] W.-Y. Keung and G. Senjanovic, Phys. Rev. Lett. **50**, 1427 (1983).

[8] D. A. Dicus, D. D. Karatas, and P. Roy, Phys. Rev. **D44**, 2033 (1991).

[9] A. Datta, M. Guchait, and A. Pilaftsis, Phys.Rev. **D50**, 3195 (1994), hep-ph/9311257.

[10] J. Almeida, F.M.L., Y. D. A. Coutinho, J. A. Martins Simoes, and M. do Vale, Phys.Rev. **D62**, 075004 (2000), hep-ph/0002024.

[11] O. Panella, M. Cannoni, C. Carimalo, and Y. N. Srivastava, Phys. Rev. **D65**, 035005 (2002), hep-ph/0107308.

[12] A. Atre, T. Han, S. Pascoli, and B. Zhang, JHEP **0905**, 030 (2009), 0901.3589.

[13] F. del Aguila, J. A. Aguilar-Saavedra, and R. Pittau, JHEP **10**, 047 (2007), hep-ph/0703261.

[14] F. del Aguila, S. Bar-Shalom, A. Soni, and J. Wudka, Phys.Lett. **B670**, 399 (2009), 0806.0876.

[15] S. Kovalenko, Z. Lu, and I. Schmidt, Phys. Rev. **D80**, 073014 (2009), 0907.2533.

[16] D. Alva, T. Han, and R. Ruiz, JHEP **02**, 072 (2015), 1411.7305.

[17] A. Das and N. Okada, Phys. Rev. **D93**, 033003 (2016), 1510.04790.

[18] C. O. Dib and C. S. Kim, Phys. Rev. **D92**, 093009 (2015), 1509.05981.

[19] E. Izaguirre and B. Shuve, Phys. Rev. **D91**, 093010 (2015), 1504.02470.

[20] S. Chakdar, K. Ghosh, V. Hoang, P. Q. Hung, and S. Nandi (2016), 1606.08502.

[21] A. Das, P. Konar, and S. Majhi (2016), 1604.00608.

[22] C. Degrande, O. Mattelaer, R. Ruiz, and J. Turner (2016), 1602.06957.

[23] P. S. B. Dev, A. Pilaftsis, and U.-k. Yang, Phys. Rev. Lett. **112**, 081801 (2014), 1308.2209.

[24] E. Ma and J. T. Pantaleone, Phys.Rev. **D40**, 2172 (1989).

[25] W. Buchmuller and C. Greub, Nucl.Phys. **B363**, 345 (1991).

[26] A. Hofer and L. Sehgal, Phys.Rev. **D54**, 1944 (1996), hep-ph/9603240.

[27] J. Peressutti, I. Romero, and O. A. Sampayo, Phys.Rev. **D84**, 113002 (2011), 1110.0959.

[28] C. Blaksley, M. Blennow, F. Bonnet, P. Coloma, and E. Fernandez-Martinez, Nucl.Phys. **B852**, 353 (2011), 1105.0308.

[29] L. Duarte, G. A. González-Sprinberg, and O. A. Sampayo, Phys. Rev. **D91**, 053007 (2015), 1412.1433.

[30] S. Antusch and O. Fischer, JHEP **05**, 053 (2015), 1502.05915.

[31] S. Bray, J. S. Lee, and A. Pilaftsis, Phys.Lett. **B628**, 250 (2005), hep-ph/0508077.

[32] J. Peressutti, O. Sampayo, and J. I. Aranda, Phys.Rev. **D64**, 073007 (2001), hep-ph/0105162.

[33] J. Peressutti and O. Sampayo, Phys.Rev. **D67**, 017302 (2003), hep-ph/0211355.

[34] V. Khachatryan et al. (CMS), JHEP **04**, 169 (2016), 1603.02248.

[35] V. Khachatryan et al. (CMS), Phys. Lett. **B748**, 144 (2015), 1501.05566.

[36] G. Aad et al. (ATLAS), JHEP **07**, 162 (2015), 1506.06020.

[37] G. Aad et al. (ATLAS Collaboration), JHEP **1110**, 107 (2011), 1108.0366.

[38] G. Aad et al. (ATLAS Collaboration), Eur.Phys.J. **C72**, 2056 (2012), 1203.5420.

[39] C. O. Dib, C. S. Kim, K. Wang, and J. Zhang, Phys. Rev. **D94**, 013005 (2016), 1605.01123.

[40] B. Batell, M. Pospelov, and B. Shuve, JHEP **08**, 052 (2016), 1604.06099.

[41] J. C. Helo, M. Hirsch, and S. Kovalenko, Phys. Rev. **D89**, 073005 (2014), 1312.2900.

[42] A. M. Gago, P. Hernández, J. Jones-Pérez, M. Losada, and A. M. Briceño, Eur. Phys. J. **C75**, 470 (2015), 1505.05880.

[43] D. G. Cerdeño, V. Martín-Lozano, and O. Seto, JHEP **05**, 035 (2014), 1311.7260.

[44] A. Blondel, E. Graverini, N. Serra, and M. Shaposhnikov (FCC-ee study Team), in *Proceedings, 37th International Conference on High Energy Physics (ICHEP 2014): Valencia, Spain, July 2-9, 2014* (2016), 1411.5230, URL `http://inspirehep.net/record/1328783/files/arXiv:1411.5230.pdf`.

[45] S. Antusch, E. Cazzato, and O. Fischer (2016), 1604.02420.

[46] L. Duarte, J. Peressutti, and O. A. Sampayo, Phys. Rev. **D92**, 093002 (2015), 1508.01588.

[47] A. A. Aguilar-Arevalo et al. (MiniBooNE), Phys. Rev. Lett. **98**, 231801 (2007), 0704.1500.

[48] A. A. Aguilar-Arevalo et al. (MiniBooNE), Phys. Rev. Lett. **102**, 101802 (2009), 0812.2243.

[49] V. G. Sinitsyna, M. Masip, and V. Y. Sinitsyna, EPJ Web Conf. **52**, 09010 (2013).

[50] S. N. Gninenko, Phys. Rev. Lett. **103**, 241802 (2009), 0902.3802.

[51] G. Aad et al. (ATLAS), Phys. Rev. **D90**, 112005 (2014), 1409.5542.

[52] G. Aad et al. (ATLAS), Phys. Rev. **D88**, 012001 (2013), 1304.6310.

[53] V. Khachatryan et al. (CMS), Phys. Lett. **B757**, 6 (2016), 1508.01218.

[54] J. Wudka, AIP Conf.Proc. **531**, 81 (2000), hep-ph/0002180.

[55] C. Arzt, M. Einhorn, and J. Wudka, Nucl.Phys. **B433**, 41 (1995), hep-ph/9405214.

[56] L. Duarte, I. Romero, J. Peressutti, and O. A. Sampayo, Eur. Phys. J. **C76**, 453 (2016), 1603.08052.

[57] A. de Gouvêa and A. Kobach, Phys. Rev. **D93**, 033005 (2016), 1511.00683.

[58] F. F. Deppisch, P. S. Bhupal Dev, and A. Pilaftsis, New J. Phys. **17**, 075019 (2015), 1502.06541.

[59] A. Das, P. S. Bhupal Dev, and N. Okada, Phys. Lett. **B735**, 364 (2014), 1405.0177.

[60] E. Fernandez-Martinez, J. Hernandez-Garcia, and J. Lopez-Pavon, JHEP **08**, 033 (2016), 1605.08774.

[61] A. Gando et al. (KamLAND-Zen), Phys. Rev. Lett. **117**, 082503 (2016), [Addendum: Phys. Rev. Lett.117,no.10,109903(2016)], 1605.02889.

[62] R. Mohapatra, Nucl.Phys.Proc.Suppl. **77**, 376 (1999), hep-ph/9808284.

[63] P. Abreu et al. (DELPHI), Z. Phys. **C74**, 57 (1997), [Erratum: Z. Phys.C75,580(1997)].

[64] D. Liventsev et al. (Belle), Phys. Rev. **D87**, 071102 (2013), 1301.1105.

[65] R. Aaij et al. (LHCb), Phys. Rev. Lett. **112**, 131802 (2014), 1401.5361.

[66] B. Shuve and M. E. Peskin (2016), 1607.04258.

[67] G. Cvetic and C. S. Kim, Phys. Rev. **D94**, 053001 (2016), 1606.04140.

[68] D. Milanes, N. Quintero, and C. E. Vera, Phys. Rev. **D93**, 094026 (2016), 1604.03177.

[69] S. Mandal and N. Sinha, Phys. Rev. **D94**, 033001 (2016), 1602.09112.

[70] C. Dib and C. S. Kim, Phys. Rev. **D89**, 077301 (2014), 1403.1985.

[71] D. Tommasini, G. Barenboim, J. Bernabeu, and C. Jarlskog, Nucl.Phys. **B444**, 451 (1995), hep-ph/9503228.

[72] F. del Aguila, J. de Blas, and M. Perez-Victoria, Phys. Rev. **D78**, 013010 (2008), 0803.4008.

[73] R. Kleiss, W. J. Stirling, and S. Ellis, Comput.Phys.Commun. **40**, 359 (1986).

[74] V. Khachatryan et al. (CMS), Phys. Rev. Lett. **114**, 061801 (2015), 1409.4789.

[75] V. Khachatryan et al. (CMS), Phys. Rev. **D91**, 052012 (2015), 1411.6977.

[76] G. Aad et al. (ATLAS), Phys. Rev. **D92**, 072004 (2015), 1504.05162.

[77] G. Aad et al. (ATLAS), Phys. Rev. **D92**, 012010 (2015), 1504.03634.

[78] J. A. Evans and J. Shelton, JHEP **04**, 056 (2016), 1601.01326.

[79] C. F. Uhlemann and N. Kauer, Nucl. Phys. **B814**, 195 (2009), 0807.4112.

[80] N. Nikiforou, Ph.D. thesis, Columbia U. (2014-02-26), URL `http://inspirehep.net/record/1296368/files/594721125_CERN-THESIS-2014-011.pdf`.